Machining parameters effects on fatigue life of Aluminium alloy aeronautical parts

Jérôme Limido, Monchai Suraratchai, Catherine Mabru, Christine Espinosa, Michel Salaün, Rémy Chieragatti

ENSICA, Département Génie Mécanique,
1 Place Emile Blouin,
31056 Toulouse Cedex 5, France

Abstract This study lies within the general scope of design and manufacturing processes improvements of aeronautical machined parts requiring fatigue behaviour guarantees. For the investigated aluminium alloy, the local stress intensity factor (K_t) has been identified as the characteristic parameter of the fatigue life. The proposed approach couples a model connecting the machining parameters with the generated surface and a fatigue model based on K_t determination by finite elements calculations. A maximum error of 15% in terms of fatigue life was obtained in the HSM milling cases studied.

1 INTRODUCTION

Fatigue life of structures is known to highly depend on the surface quality. Consequently, a great attention is paid to the specification and the realization of surfaces of machined parts when those must be dimensioned in fatigue. Three surface parameters are usually proposed to describe surface condition: i) a geometrical parameter: surface roughness; ii) a mechanical parameter: residual stress; iii) a metallurgical parameter: microstructure. These parameters can vary separately according to the machining conditions. In engineering design, the effects of these parameters are commonly accounted for by using empirical reduction factors which modify the endurance limit of the material. Reduction factors are defined for each type of machining process. Moreover, within each category of machining process the use of these reduction factors leads to surface specifications (generally in terms of roughness) linked to machining parameters such as tool shape, feed rate… Even if giving satisfactory fatigue life predictions, the use of this empirical method has obviously limitations due to its restricted area of validity. Indeed, changing machining process or machining parameters must then be accompanied by a new definition of reduction factors and/or surface specifications that must be validated by performing new fatigue tests. This constitutes a real problem as machining processes are in constant evolution in order to increase productivity.

In this context, the present study proposes an approach to directly connect machining parameters to fatigue life without performing time-consuming and expensive tests for an aeronautical aluminium alloy. The objective here is to give tendencies on the machining parameters influence on fatigue life. In this aim, the work has been divided in three main parts. In the first part (section 2), the surface quality criteria related to fatigue resistance is identified for the investigated alloy. It appears that surface texture, by generating local surface stress concentration, is the predominant parameter governing fatigue strength. The stress concentration factor K_t is calculated by finite element analysis from surface measurements. This so-calculated stress concentration factor is integrated in two different modelling to predict limited fatigue lives and fatigue limit. The second part (section 3) is devoted to the modelling of the surface generation from machining parameters. This work leads to predict a surface topography that can be directly used in the previous modelling. Such coupling between both approaches is presented in section 4. In this last part predicted fatigue lives are confronted with experimental results.

2 SURFACE QUALITY CRITERIA ON THE FATIGUE RESISTANCE OF 7010 AL ALLOY

2.1 Criteria identification

The material investigated in this paper is a 7010-T7451 aluminium alloy, Al Zn6MgCu as defined by ISO norms. It was provided in the form of a rolled plate of 70mm thickness. The microstructure is composed of grains that are highly elongated in the rolling direction. Grain size is about 350µm in the rolling (L) direction and about 150µm and 60µm in transverse TC and TL directions respectively. Al_7Cu_2Fe and Mg_2Si intermetallic particles of 8-10µm size can be found regularly in the microstructure and are located in recrystallized grains.

These grains are smaller than the previous grains: 80, 60 and 40 µm in L, TL and TC directions respectively. Specimens are taken in the plate so that the stress induced by four-point bending is parallel to the TL direction. They have been machined according to different machining conditions in order to obtain different surface conditions in terms of roughness and residual stresses. Residual stresses have been measured using X-ray diffraction technique with ASTX2001 device. The so-obtained values of residual stresses are given within +/- 30MPa. Concerning the geometrical characterization of the surfaces, a Mahr (Perthometer PKG-120) contour and roughness measuring system has been used. Surface characteristics are presented in Table I. Whatever the machining process and machining parameters, no change of the surface microstructure has been detected with the means of investigation that were used (microscopic observation and micro-hardness measurements). Four-point bending fatigue tests have been conducted at room temperature in order to explore fatigue lives around 10^5 cycles. Tests were performed with a load ratio R=0.1 and a frequency of 10Hz.

Table I. Surface characteristics of four-point bending specimens

Specimen reference	Machining	Ra* (µm)	Rt*(µm)	Transversal Residual Stress (MPa)	Longitudinal Residual Stress (MPa)
UL11	shaper	0.5	3	-137	-191
UL12	shaper	0.5	3	-45	-78
UL21	shaper	7	30	-54	-157
UL22	shaper	7	30	-21	-147
Fine milled	HSM milling	0.25	1.7	-	-
Slot milled	HSM milling	11.1	40	-	-

* Ra and Rt as defined in ISO 4287

Experimental SN curves are presented in Figure 1. The influence of surface condition on the fatigue life is more important for high cycle fatigue (N_f>3.10^5 cycles). Roughness has obviously a predominant influence on the fatigue life. For a given roughness, residual stresses only seem to have a slight influence on the fatigue life: UL11 and UL12 display the same fatigue behaviour. However, the geometric roughness parameter R_a is not able to fully explain the difference in fatigue strength between all the samples: for instance, slot milled specimens exhibit a better fatigue resistance than UL21 and UL22 specimens in spite of a higher value of R_a.

Fracture surfaces observations show that whatever the specimen and the load level, fatigue cracks initiated on microstuctural defects (essentially intermetallic inclusions and sometimes porosity). This is consistent with the observations that can be found in literature [1]. These defects were included in small recrystallized grains.

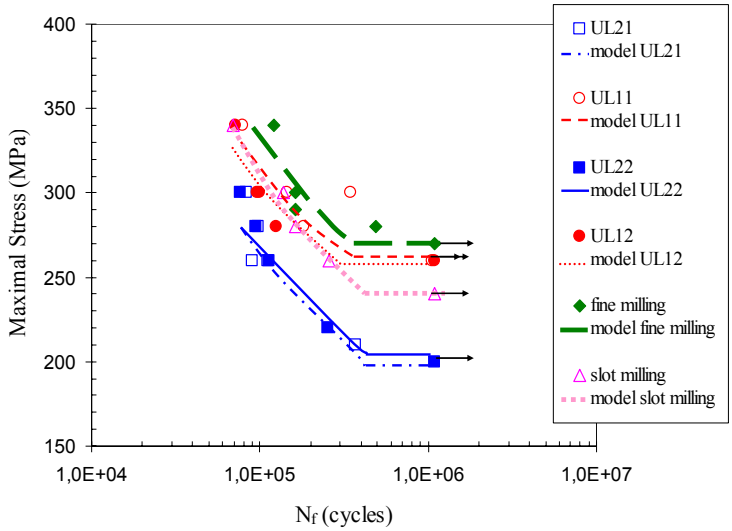

Figure 1. Predicted fatigue life time compared to experimental SN curves

2.2 Modelling the influence of surface texture

As presented in the previous section and noted also by many authors [2-4], standard purely geometric surface roughness parameters are not able to correctly describe the effect of roughness on the fatigue life of the investigated aluminium alloy. In the following, surface roughness is supposed to generate local stress concentration. However, this effect is not considered in terms of notch effect through the fatigue stress concentration factor K_f but is integrated in a fracture mechanics modelling.

2.2.1 *Finite element analysis of surface topography*

In most of the recent approaches presented in the literature [2,4,5], the stress concentration factor K_t is calculated from averaged geometrical parameters of the surface. In the present study, the estimate of K_t based on measurements of the surface topography has been preferred. K_t is found by finite element analysis of the measured surface topography and is then supposed to lead to a stress condition which is more representative of what really undergo the samples. This way of characterizing a surface texture from a mechanical point of view without the use of geometrical parameters gave place to a patent [6]. A similar approach has also been proposed by As et al. [3]. 2D profiles that are measured are recorded with a sampling rate of 1µm/point. From the 17000 points that are recorded, only 800 points are regularly extracted and interpolated with a spline function to be used in the finite element modelling. As seen in Figure 2, this results in a filtered profile where second order roughness (induced by tool edge defects for instance) is not taken into account. This filter has been chosen because stress concentration generated by second order roughness is supposed to be not relevant compared to stress concentration generated by first order roughness (due to tool shape and machining parameters). This profile is then used as surface model to generate the finite element geometry. Material behaviour is linear elastic. Plane strain hypothesis is supposed for this 2D calculation. Triangular elements with quadratic interpolation are used for the mesh. Elements size is roughly 30µm. For this filtered profile, it has been shown this mesh size leads to convergence of the numerical results. Problems of validity of continuum mechanics and of the hypothesis of isotropic and homogeneous material induced by extremely refined mesh, such as pointed out by As et al. [3], are so avoided. Uniform load is applied as boundary conditions. The maximal stress obtained by the calculation is then divided by the nominal stress due to the applied load to classically determine the stress concentration factor K_t. An example of finite element calculation performed to determine K_t is shown in Figure 3.

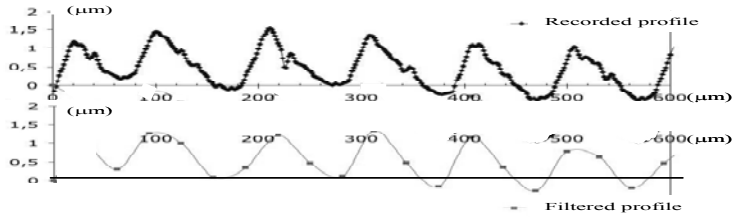

Figure 2. Example of recorded and filtered profile of surface specimen

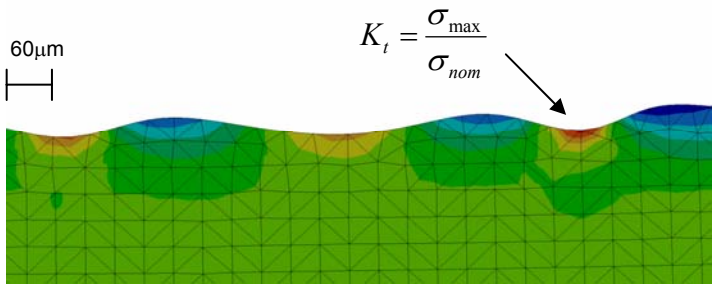

Figure 3. Example of finite element calculation to determine stress concentration factor

2.2.2 *Effect of local stress concentration*

As noticed in section 2.1., the effect of surface roughness is different according to fatigue life time. Therefore, two different modelling are proposed to predict fatigue behaviour for N_f higher and lower than 3.10^5 cycles. For N_f higher than 3.10^5 cycles the chosen model relies on the non propagation of an initial crack (or defect). According to linear elastic fracture mechanics the fatigue crack propagation threshold can be expressed with the following equation:

$$\Delta K_{th} = F\Delta\sigma_{th}\sqrt{\pi a} \tag{1}$$

where a is the crack length, F is a shape factor and $\Delta\sigma_{th}$ is the minimum stress range required to propagate such a crack. Supposing the initial crack is located at the bottom of a machining groove and is very small, the stress concentration effect affecting the stress at the crack tip leads to

$$\Delta K_{th} = FK_t\Delta\sigma_{app}\sqrt{\pi a} \tag{2}$$

The fatigue limit can then be derived by considering it as the minimum stress range that can be applied without involving any propagation of an initial defect:

$$\Delta\sigma_D = \frac{\Delta K_{th}}{FK_t\sqrt{\pi a}} \tag{3}$$

With the following hypotheses, the fatigue limit is then quite easy to evaluate and only depends on the stress concentration factor:

1. the threshold stress intensity factor range ΔK_{th} does not depend on the surface condition as whatever the machining parameters, metallurgical evolution has not been detected for the investigated alloy. Its value can be found in data base (ΔK_{th}=3.5MPa $m^{1/2}$) [7].
2. Initial crack or defect does not depend on the surface condition. Indeed, as noted in section 2.1., failure initiation always occurred on intermetallic inclusion within a re-crystallized grain, whatever the surface conditions. According to these observations, initial crack (defect) length a is considered to be the re-crystallized grain size in TC direction, that is to say 40µm. In the same way, the shape factor F is supposed to be identical whatever the surface condition and is roughly 1.12 for small cracks [8].

For N_f lower than 3.10^5 cycles, the roughness effect is different than for N_f higher than 3.10^5 cycles. This is attributed to crack propagation which constitutes the main part of fatigue life time. Machining process and subsequent roughness only have influence on the crack propagation in surface. Therefore, crack propagation in surface (along L direction) and in depth (along TC direction) are treated separately. In the case of a semi elliptical crack the stress intensity factor can be expressed according to Newman and Raju [8]:

$$K_{I\phi} = f(a,c,\phi,W,t)\sigma\sqrt{\pi a} \tag{4}$$

where a and c are respectively the half short axis length and half long axis length of the crack, ϕ is the angle (compared to the long axis) for which K is calculated, W is the specimen width and t the specimen thickness. The detailed expression of f function can be found in [8]. It is supposed that a crack propagates in surface (increasing c) and in depth (increasing a) according to Paris law:

$$\frac{da}{dN} = C(\Delta K_{90°})^m \qquad \frac{dc}{dN} = C(\Delta K_{0°})^m \tag{5}$$

with C and m material constants that can be found in database (m=3.41, C=3.17 10^{-11} m/cycle in our case). The main hypothesis is then that surface roughness generates stress concentration that only alters the surface crack propagation and the Paris law becomes:

$$\frac{da}{dN} = C(\Delta K_{90°})^m \qquad \frac{dc}{dN} = C(K_t\Delta K_{0°})^m \tag{6}$$

An iterative calculation is then performed and, for each cycle, a and c are calculated and their new values are used to evaluate $\Delta K_{90°}$ and $\Delta K_{0°}$. Initial crack size is re-crystallized grain size with an elliptical shape ratio a/c=0.5 according to fracture surfaces observations. Calculation is stopped when either $a=t$, $c=W$ or $K_\phi=K_{IC}$ that is to say when crack either propagates through the thickness, through the width or is unstable. The crack propagation life (N_p) can then be evaluated if the stress concentration factor associated with surface roughness is known. Afterwards an estimate of the crack initiation life (N_i) can be obtained using a reference SN curve. Considering total life time is the sum of crack propagation life time and crack initiation life time, N_i is estimated from the experimental total life time and the previous calculated crack propagation life time with the appropriate stress concentration factor. It is then assumed that the crack initiation life time can be expressed according to a Basquin type law [9]:

$$N_i = \beta(K_t\sigma)^\alpha \tag{7}$$

β and α are easily determined from a reference curve and Eq.(7) can be applied whatever the specimen.

For each specimen, the stress concentration factor K_t characterising the surface conditions is calculated according to the previous process presented in section 2.2.1. The so-obtained values are then used in Eq. (3) to determine the fatigue limit of each type of specimen. For fatigue lives lower than 3.10^5 cycles, the total number of cycles to failure is calculated with

$$N_f = N_i + N_p \tag{8}$$

where N_i is determined via Eq. (7) and N_p is estimated by the iterative calculation using Eq. (6). The so-obtained results are compared with experimental data in the SN curves presented in Figure 1. Fatigue limits are also included to get a global assessment of the complete modelling. Experimental results and predicted fatigue life time are in good agreement for all types of specimens. The whole approach has been validated with other high speed machined specimens by Suraratchai [10].

3 MODELLING MACHINED SURFACE AND CUTTING FORCES

The approach proposed in section 2.2. is based on the surface texture influence on fatigue behaviour. Thus the next step to achieve a predictive tool able to connect machining parameters to fatigue life is to develop a model predicting surface texture. The model presented here takes into account the ideal shape of the tool with first order runout and tool deflection caused by the cutting forces. Vibrations phenomena are not studied.

Most of the studies concerning cutting modelling deal with orthogonal cutting [11]. Indeed, this framework allows a 2D plane strain modelling and a better comprehension of the basic mechanisms of chip formation. For fifteen years, many finite elements calculation models have been developed for this purpose, but their extension to 3D industrial cases (milling for example) remains very complex and very expensive in terms of computing time [11]. To mitigate this problem, the approach proposed in the present paper is based on a 3D mechanistic model developed by Altintas et al. [12]. This model connects chip thickness to cutting forces via cutting coefficients that are experimentally obtained by series of orthogonal cutting tests. In the present approach, these machining tests are replaced by 2D numerical tests using a SPH model. In addition, the local thickness of not deformed chip is calculated by the means of a Z-Map intersection algorithm [13]. This algorithm allows the modelling of complex cases of millings (5 axis hemispherical milling for example) as well as the rebuilding of the machined surface topography. Besides, in the present study, the interaction between cutting forces calculation and surface building is introduced. Tool bending which may highly influence surface topography is therefore taken into account. The modelling principle is summarized in Figure 4.

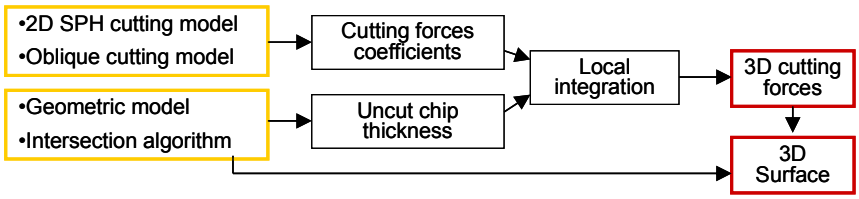

Figure 4. Modelling principle

3.1 2D SPH numerical modelling

Numerical calculations have been completed using a Smoothed Particle Hydrodynamics (SPH) method in the frame of the Ls-Dyna FE hydrodynamic code [14]. SPH is a meshfree method which proposes a new spatial discretization: the points or particles are characterized by a mass and an influence sphere where the interactions with neighbour particles are weighted by smoothing functions. The use of this method for the modelling of cutting offers numerous advantages: high strains are easily handled (no re-meshing is needed), the chip/workpiece separation is “natural” and friction is implicitly taken into account through particles interaction. Therefore the friction parameter is not used as an adjusting numerical parameter; which is generally the case in more classical finite element methods. The material constitutive model proposed by Johnson and Cook [15] is used. The validation of this approach has been carried out for 2D orthogonal cutting by comparing numerical results with experimental results in terms of chip morphology and cutting forces by Limido et al.[16].

3.2 Cutting coefficients

In order to determine the cutting coefficients which are required in the mechanistic model, the influence of feed on the cutting forces and feed forces has been studied with the developed SPH model. An example of results obtained for a titanium alloy Ti6Al4V (experimental data from [12]) is presented in Figure 5.

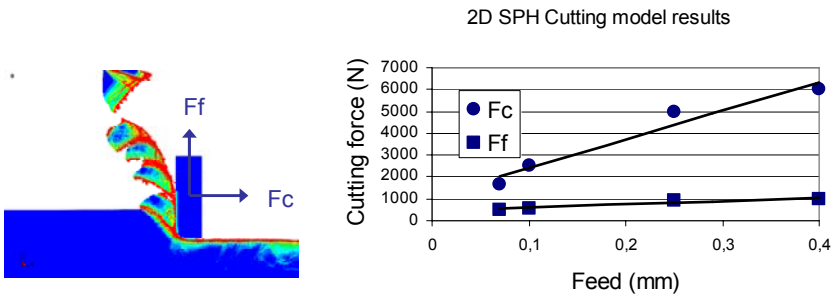

Figure 5. SPH results: influence of feed on cutting forces

The four orthogonal cutting coefficients are then deduced from these two curves (two origin ordinates, two slopes). In the case of milling, cutting conditions on the cutting edge are not orthogonal but oblique. A traditional empirical transformation [11] transforms the 4 coefficients of orthogonal cutting into 6 coefficients of oblique cutting. They are function of the angle between tool speed and tool edge. It is then possible to calculate the forces as a function of local 3D cutting conditions.

3.3 Intersection tool/workpiece modelling

The last data to be determined in order to use the mechanistic model is the local thickness of not deformed chip. Analytical models exist but are limited to basic machining processes. A Z-Map approach [13] has been selected because it applies to a large variety of milling types. This method is based on a vectorial representation of the workpiece: the passage of the edge cuts a certain number of vectors to a certain height and this, at each step of rotation. It is then possible to determine the 3D texture of the machined surface as well as the local cutting conditions. This model is developed within the framework of a static and ideal approach of the tool feed. Nevertheless, taking into account the characteristic defects of the modelled tool is necessary. Indeed, these defects have little influence on the process (cutting forces…) but much more on the texture of the generated surface. The implemented model thus takes into account the axial, radial and eccentricity defects of the milling cutter. The path of the cutting edge is discretized for each step of rotation. Determining the quantity of removed material is then possible with an intersection algorithm. This phase is illustrated by the intersection of an increment of rotation with a vector of the Z-map. The update of 3D texture of the workpiece then follows.

The validation of this model has been carried out with hemispherical milling cases. Figure 6 shows the good agreement between numerical surface and measured surface. The influence of feed per tooth on the geometrical roughness parameter R_z is also presented in this figure. With this model it is also possible to build surfaces generated by parallel ends cutter, torus cutter, ball cutter, and insert cutter.

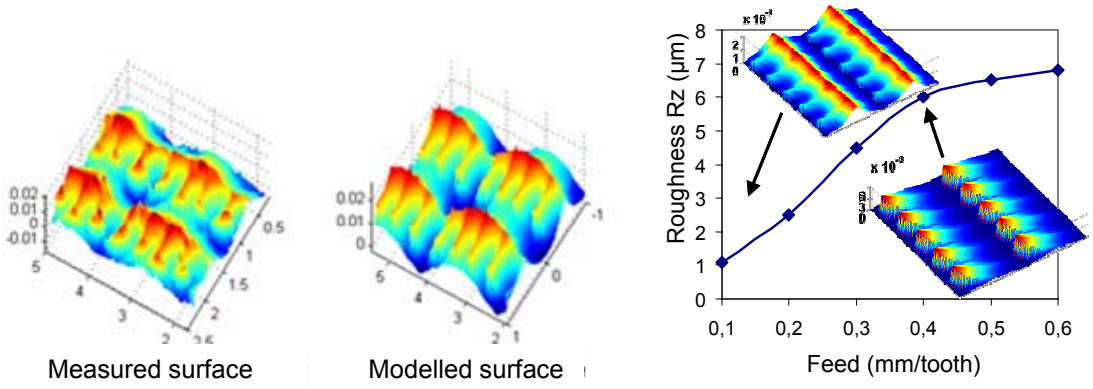

Figure 6. Surface generation modelling: a) comparison with experimental measurements b) influence of feed on surface roughness

3.4 Cutting forces

The mechanistic model of Altintas et al. [12] proposes to discretize the cutting edge in a series of elementary edges. The total cutting force is then the sum of all the cutting forces of these elementary edges. These elementary cutting forces are obtained by multiplying the elementary chip thickness (provided by the intersection tool/workpiece modelling of the previous section) by the cutting coefficients which are determined from 2D SPH numerical simulations (section 3.2.). In Figure 7, results from the present model are compared with experimental data from the literature [12] in the case of hemispherical milling of Ti6Al4V. It clearly appears that this model is able to calculate cutting forces for 3D applications with a very good precision.

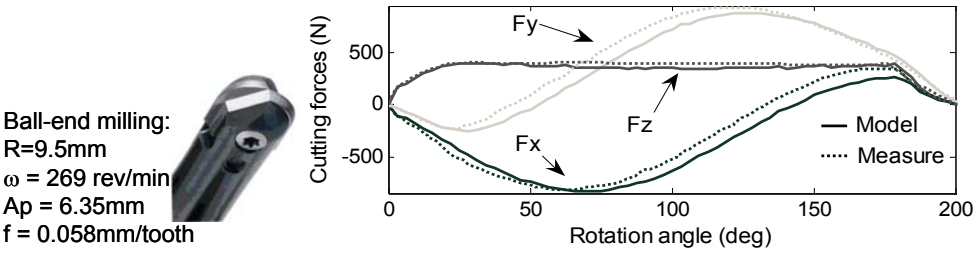

Figure 7. Comparison between calculated and experimental cutting forces (hemispherical milling)

4 FATIGUE LIFE PREDICTION FROM MACHINING PARAMETERS

With the previous model presented in section 3, it is possible to predict machined surface topography from machining parameters. This model takes into account axial, radial and eccentricity defects of milling cutters and can also integrate the bending of the tool as cutting forces are also calculated. In section 2, it has been proved that surface topography is the predominant surface parameter affecting fatigue life for the investigated Al alloy. The implementation of the model connecting the machining parameters to generated surface coupled with the $K_t \rightarrow N_f$ method of section 2 thus makes it possible to consider a predictive approach of the relationship machining parameters – fatigue life. Actually, we propose to replace the surface topography measurement by the result of the surface modelling to calculate the stress concentration factor K_t. The finite element analysis of the surface profile is then performed like for the measured one as presented in section 2.2.1. The objective here is to give tendencies on the machining parameters influence on fatigue life.

This approach has been validated by comparison with fatigue tests completed with 4 point bending specimens machined by high speed milling with torus cutter. The results are presented in Figure 8. The model predicts the fatigue life with a maximal error of 15% for the nine HSM milling cases that were studied. A strong concentration of predicted fatigue lives around 90000 cycles can be pointed out. This is due to the slight variations of the machining parameters for these various cases. Nevertheless, as seen in Figure 9 for hemispherical milling, a strong evolution of predicted fatigue life can be noticed when considering a large variation of the machining parameters. The machining of fatigue specimens with these machining conditions would allow a comparison between tests and model results in terms of fatigue life. This work is under development.

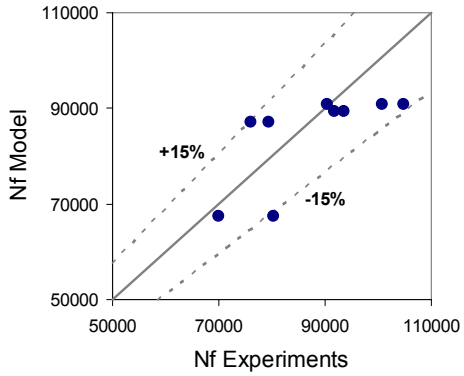

Figure 8. Comparison of predicted and experimental fatigue life time for HSM specimens

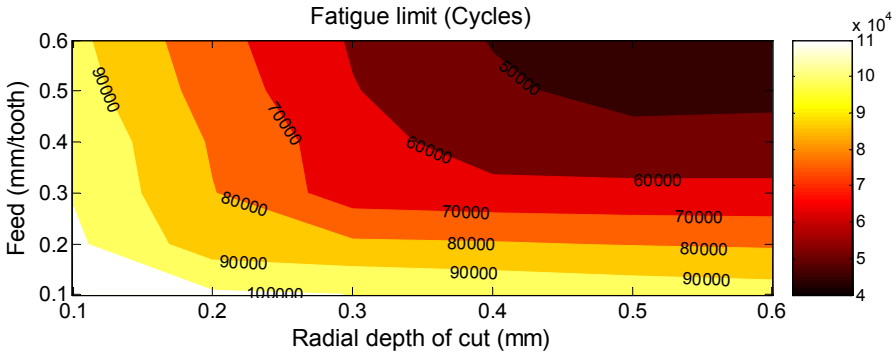

Figure 9. Predicted influence of feed and radial depth of cut on fatigue life for hemispherical milling

5 CONCLUSION

For the present Al alloy, it has been proved that surface topography is the predominant surface parameter affecting fatigue life. In order to model this effect, surface topography is characterized from a mechanical point of view without the use of geometrical parameters: stress concentration factor K_t is initially calculated by finite element analysis from surface measurements. This so-calculated stress concentration factor is integrated in two different modelling to predict limited fatigue lives and fatigue limit. In addition to this calculated K_t, these two modelling only require basic fatigue crack propagation data (fatigue threshold and Paris law parameters). As shown by the relevance of the results compared to experimental ones, this first approach (measurement of surface topography, determination of K_t, fatigue life prediction) gives a reliable mean to predict fatigue life when changing machining parameters. In order to provide a predictive tool, a complete modelling of surface generation is then developed coupling a 2D SPH orthogonal cutting model, a Z-Map intersection tool/workpiece model and a 3D mechanistic model. Input data for this 3D surface prediction are limited to a Johnson-Cook

material constitutive model and geometrical description. This "numerical" surface is then used as the measured one to calculate K_t and predict fatigue life. The whole model is described in Figure 10. The first results are in good agreement with experimental results with a maximal error of 15%. The combined approach (from machining parameters to fatigue life) appears to be a useful predictive tool which is able to give tendencies on the machining parameters influence on fatigue life of 7010 Al alloy.

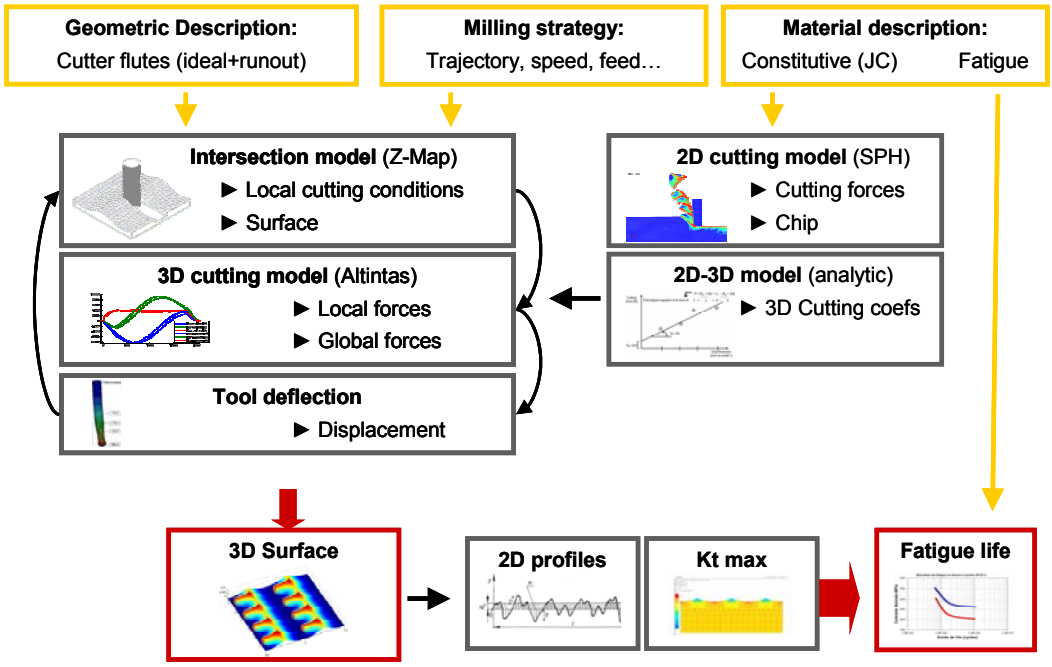

Figure 10. Principle of the predictive modelling from machining parameters to fatigue behaviour

6 ACKNOWLEDGMENT

This study was carried out as part of a common research program in partnership with AIRBUS France.

7 REFERENCES

1. G. Patton, C. Rinaldi, Y. Bréchet, G. Lormand, R. Fougères, *Mat. Sci. Eng. A*, 254, 1998, 207-218.
2. D. Arola , C.L. Williams, *Int. J. Fatigue*, 24, 2002, 923-930.
3. SK. As, B. Skallerud, B.W. Tveiten, B. Holme, *Int. J. Fatigue*, 27, 2005, 1590-1596.
4. S. Andrews, H. Sehitoglu, *Int. J. Fatigue*, 22, 2000, 619-630.
5. D. Arola, M.Ramulu, *J. Compos. Mater.,* 33(2), 1999, 101-186.
6. R. Chieragatti, M. Surarachai, C. Mabru, C. Espinosa, V. Vergnes, Procédés de caractérisation de la tenue en fatigue d'une pièce à partir de son profil de surface, French Patent n°0650793, 2006.
7. V. Zitounis, P.E. Irving, *Int. J. Fatigue,* 29(1), 2007, 108-118.
8. J.C. Newman, I.S. Raju, Stress intensity factor equations for cracks in three dimensional finite bodies subjected to tension and bending loads, NASA Technical Memorandum, 1984.
9. C. Bathias, J.P. Baïlon, La fatigue des matériaux et des structures, 2nd edition. HERMES editor. Paris, 1997, 106.
10. M. Suraratchai, Influence de l'état de surface sur la tenue en fatigue de l'alliage d'aluminium 7010, PhD thesis, Université Toulouse III, 2006.
11. M.C. Shaw, Metal cutting principles, Oxford university press, 2004.
12. P. Lee, Y. Altintas, *Int. J. Mach. Tools Manufact*., 36(9), 1996, 1059-1072.
13. Y. Takeuch, M. Sakamoto, Y. Abe, R. Orita, Annals of the CIRP, 38, 1995, 429-432.
14. Livermore Software Technology Corporation, LS-DYNA theory manual, ISBN 0-9788540-0-0, 2006
15. G.R. Johnson, W.H. Cook, Proceedings of the 7th international symposium on ballistics, 1983, 541-547
16. J. Limido, C. Espinosa, M. Salaün, J.L. Lacome, *Int. J. Mech. Sci*., 49, 2007, 898-908.